MINIMIZING A WEIGHTED ERROR CRITERION FOR SPATIAL ERROR CONCEALMENT OF MISSING IMAGE DATA

Katrin Meisinger and André Kaup

Chair of Multimedia Communications and Signal Processing,
University of Erlangen-Nuremberg
Cauerstr. 7, 91058 Erlangen, Germany
{meisinger,kaup}@LNT.de

ABSTRACT

In this contribution we present an algorithm for spatial error concealment of lost image data caused by transmission of images in error prone environments. The surrounding correctly received image signal is approximated by a weighted linear combination of basis functions and the missing image data is obtained by a frequency selective extrapolation. During the approximation a novel weighted error criterion is minimized. We use an isotropic correlation model for the weighting function taking the correlation among pixels into account and emphasizing pixels wich are closer to the missing area. 2D DFT basis functions are especially suited for the signal extrapolation in order to be able to reconstruct monotone areas, edges and noisy regions and allow an efficient realization of the algorithm in the frequency domain. Due to the weighting function we could improve the concealing performance of the algorithm considerably while halving the required FFT size.

1. INTRODUCTION

Images or videos coded by block based techniques like JPEG or MPEG may suffer from block loss in erroneous transmission. Thus, error concealment at the decoder side has to be applied. Two approaches are known in error concealment. Spatial error concealment on the one hand uses the surrounding correctly received image information. On the other hand temporal error concealment exploits motion information. Spatial error concealment is applied in image transmission and intraframe coded video transmission.

Wang et. al assume that the image content is changing smoothly [1]. This standard approach tries to restore the transition across the block boundary as smooth as possible. The sequential method of [2] predicts each pixel from the available next neighbors. The lost block is reconstructed pixel by pixel from eight directions and given by a weighted linear combination of these reconstructed blocks requiring thus an extensive computational load.

Further, the methods described in [3], [4], [5] and [6] are also compared for evaluation purposes. The algorithm proposed in [6] uses a frequency selective extrapolation method in order to conceal lost blocks. The concealing performance of [6] could be improved significantly by introducing a novel weighted error criterion.

2. SIGNAL APPROXIMATION BY SUCCESSIVE APPROXIMATION

Fig. 1 describes schematically the situation after a block loss has occurred. The area $\mathcal{L}$ consists of the gray area $\mathcal{A}$ made up of the known surrounding blocks and the white area $\mathcal{L}\backslash\mathcal{A}$ being the lost block. The concealment algorithm works as follows: the known surrounding is approximated by a linear discrete approximation and the missing block is then given by a signal extrapolation.

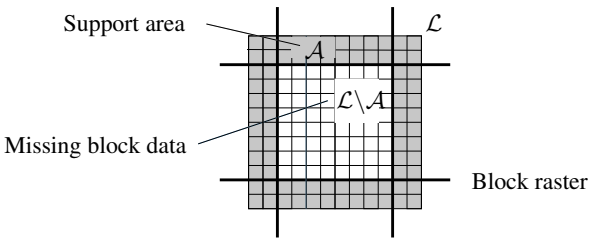

Fig. 1. The known area $\mathcal{A}$ (gray) is approximated by a parametric model and the missing $\mathcal{L}\backslash\mathcal{A}$ (white) obtained by extrapolation.

More precisely, the gray values $f[m,n]$ of the original signal existing only within $\mathcal{A}$ at row m and column n are approximated by a parametric model $g[m,n]$ defined on $\mathcal{L}$. The parametric model is a weighted linear combination of basis functions. We choose two-dimensional DFT basis functions due to their convincing signal extrapolation properties (see [6])

$$\varphi_{k,l}[m,n] = \mathrm{e}^{j\frac{2\pi}{M}mk}\mathrm{e}^{j\frac{2\pi}{N}nl}. \tag{1}$$

In order to approximate the support area, we evaluate an error criterion $E_{\mathcal{A}}$ between the original signal and the parametric model. Since the direct least-squares approach by minimizing the error criterion does not lead to a unique solution [6], an iterative algorithm is applied.

The parametric model in iteration ν is given by

$$g^{(\nu)}[m,n] = \frac{1}{2MN}\sum_{(k,l)\in\mathcal{K}_\nu}(c_{k,l}^{(\nu)}\,\varphi_{k,l}[m,n] + c_{M-k,N-l}^{(\nu)}\,\varphi_{M-k,N-l}[m,n]) \tag{2}$$

with $c_{k,l}^{(\nu)}$ denoting the complex expansion coefficients and $\mathcal{K}_\nu$ the set of used basis functions. The area $\mathcal{L}$ consists of $M \times N$ pixels which is also the number of available basis functions.

The image signal and its parametric model are real signals and therefore it holds

$$c_{M-k,N-l}^{(\nu)} = c_{k,l}^{(\nu)*} \text{ as well as} \tag{3}$$
$$\varphi_{M-k,N-l}^{*}[m,n] = \varphi_{k,l}[m,n]. \tag{4}$$

This iterative algorithm uses the principle of successive approximation and computes one expansion coefficient and its conjugate complex counterpart per iteration. The support area is thus de-

0-7803-8554-3/04/$20.00 ©2004 IEEE.

scribed by a few dominant features, more precisely a weighted linear combination of a few selected basis functions. An iteration incorporates 2 steps. First of all, a suitable basis function is selected and then the respective expansion coefficient is updated.

With the help of a binary window function $w[m,n]$ being one only for available pixels

$$w[m,n] = \begin{cases} 1 & , \quad m,n \in \mathcal{A} \\ 0 & , \quad m,n \in \mathcal{L}\backslash\mathcal{A} \end{cases} \tag{5}$$

we can express the residual error in the support area by

$$r^{(\nu)}[m,n] = (f[m,n] - g^{(\nu)}[m,n]) \cdot w[m,n]. \tag{6}$$

The residual error in the next iteration $\nu+1$ is obtained by further approximating the residual error in the known area by a weighted suitable basis function

$$\begin{aligned} r^{(\nu+1)}[m,n] &= r^{(\nu)}[m,n] - \\ \frac{1}{2MN}&\left(\Delta c \varphi_{u,v}[m,n] + \Delta c^* \varphi_{M-u,N-v}[m,n]\right) \cdot w[m,n]. \end{aligned} \tag{7}$$

2.1. Coefficient Update

First of all we derive the computation of the expansion coefficient $c_{u,v}^{(\nu+1)}$ (and thus also $c_{M-u,N-v}^{(\nu+1)}$) in iteration $\nu+1$ assuming a suitable basis function with index u,v has already been selected.

With help of the weighting function $\widetilde{w}[m,n]$ having only non-zero amplitudes $\rho[m,n]$ in the support area

$$\widetilde{w}[m,n] = \begin{cases} \rho[m,n] & , \quad m,n \in \mathcal{A} \\ 0 & , \quad m,n \in \mathcal{L}\backslash\mathcal{A}. \end{cases} \tag{8}$$

we introduce a novel weighted error criterion

$$\begin{aligned} \widetilde{E}_{\mathcal{A}}^{(\nu)} = \sum_{(m,n)\in\mathcal{L}} \widetilde{w}[m,n] \Big(r^{(\nu)}[m,n] - \\ \frac{1}{2MN}(\Delta c \varphi_{u,v}[m,n] + \Delta c^* \varphi_{M-u,N-v}[m,n]) w[m,n] \Big)^2 \end{aligned} \tag{9}$$

Thus, in contrary to [6], we minimize a weighted error criterion during the approximation and are therefore able to assign more importance to certain areas during the approximation. It is minimized by taking the derivative with respect to Δc and setting it to zero using $\widetilde{w}[m,n] \cdot w[m,n] = \widetilde{w}[m,n]$ which yields

$$\begin{aligned} \Delta c \sum_{(m,n)\in\mathcal{L}} \widetilde{w}[m,n] \varphi_{u,v}[m,n] \varphi_{M-u,N-v}[m,n] + \\ \Delta c^* \sum_{(m,n)\in\mathcal{L}} \widetilde{w}[m,n] \varphi_{M-u,N-v}[m,n] \varphi_{M-u,N-v}[m,n] \\ = 2MN \sum_{(m,n)\in\mathcal{L}} \widetilde{w}[m,n] r^{(\nu)}[m,n] \varphi_{M-u,N-v}[m,n]. \end{aligned} \tag{10}$$

Analogously, a conjugate complex equation to (10) is obtained.

The coefficient update $c_{u,v}^{(\nu+1)}$ is thus performed by modification of $c_{u,v}^{(\nu)}$ by Δc

$$c_{u,v}^{(\nu+1)} = c_{u,v}^{(\nu)} + \Delta c \tag{11}$$

$$c_{M-u,N-v}^{(\nu+1)} = c_{M-u,N-v}^{(\nu)} + \Delta c^* \tag{12}$$

The conjugate complex coefficient is updated due to symmetry requirements.

The index u,v is included in the set of selected basis functions

$$\mathcal{K}_{\nu+1} = \mathcal{K}_\nu \cup \{u,v\} \quad \text{if} \quad u,v \notin \mathcal{K}_\nu. \tag{13}$$

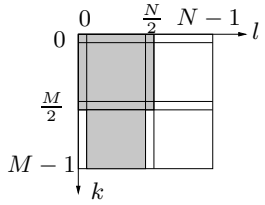

Fig. 2. Search area for DFT basis functions

2.2. Selection of Suitable Basis Function

In the following the selection of a suitable basis function is derived. We select that basis function which is minimizing the weighted residual error criterion from iteration ν to $\nu+1$. Hence, we establish this equation taking into account that the residuum $r^{(\nu)}[m,n]$ is orthogonal to the selected basis function:

$$\begin{aligned} \sum_{(m,n)\in\mathcal{L}} \widetilde{w}[m,n](r^{(\nu+1)}[m,n])^2 = \sum_{(m,n)\in\mathcal{L}} \widetilde{w}[m,n](r^{(\nu)}[m,n])^2 - \\ \frac{1}{(2MN)^2} \sum_{(m,n)\in\mathcal{L}} \widetilde{w}[m,n] \left(\Delta c \varphi_{u,v}[m,n] + \Delta c^* \varphi_{M-u,N-v}[m,n]\right)^2. \end{aligned} \tag{14}$$

In other words that basis function with index u,v is selected which is maximizing the reduction of the error criterion

$$\begin{aligned} \Delta\widetilde{E}_{\mathcal{A}}^{(\nu)} = \frac{1}{2(MN)^2} \Bigg(|\Delta c|^2 \sum_{(m,n)\in\mathcal{L}} \widetilde{w}[m,n] \varphi_{u,v}[m,n] \varphi_{u,v}^*[m,n] \\ + \quad \mathrm{Re}\{\Delta c^2 \sum_{(m,n)\in\mathcal{L}} \widetilde{w}[m,n] (\varphi_{u,v}[m,n])^2\} \Bigg) \end{aligned} \tag{15}$$

However, the search area for selecting a basis function is limited to the gray area in Fig. 2 due to symmetry requirements (3), (4).

The algorithm is initialized by

$$g^{(0)}[m,n] = 0. \tag{16}$$

The algorithm terminates when $\Delta\widetilde{E}_{\mathcal{A}}^{(\nu)}$ drops below a prespecified threshold ΔE_{min}.

2.3. Concealment by Signal Extrapolation

So far the approximation of the known area by a weighted linear combination is described. Hence, the parametric model defined on $\mathcal{L}$ is given by the signal extrapolation according to (2). Finally, the missing block is obtained by cutting it out of $g[m,n]$.

3. IMPLEMENTATIONAL ISSUES

In this section we treat implementational issues. All derivations are done so far by a series expansion in the spatial domain which is computationally extensive like the evaluations of the sums in (15). Our goal is to express all equations in the frequency domain. But before we concentrate on the frequency domain representations, we deal with algorithmical simplifications being necessary due to the novel weighting function.

3.1. Algorithmical Simplifications

The derivations in Sec. 2 depend on the weighting function $\widetilde{w}[m,n]$ and window function $w[m,n]$. In the following we simplify these equations such that they only depend on $\widetilde{w}[m,n]$. The coefficient update involves the evaluation of $\widetilde{w}[m,n] r^{(\nu)}[m,n]$ according to (10). However, the residuum $r^{(\nu)}[m,n]$ inserted in (10) after transition from $\nu+1$ to ν is equal to the residuum $r^{(\nu+1)}[m,n]$ of (7)

cut to the support area with help of $w[m,n]$. Instead of inserting $r^{(\nu)}[m,n]$ in (10) and weighting it, we already insert the weighted residual error and change (7) to

$$\widetilde{w}[m,n]r^{(\nu+1)}[m,n] = r_{\widetilde{w}}^{(\nu+1)}[m,n] = \widetilde{w}[m,n]\left(r^{(\nu)}[m,n] - \frac{1}{2MN}\left(\Delta c\varphi_{u,v}[m,n] + \Delta c^{*}\varphi_{M-u,N-v}[m,n]\right)\right) \quad (17)$$

and also rewrite (6) accordingly

$$r_{\widetilde{w}}^{(\nu)}[m,n] = (f[m,n] - g^{(\nu)}[m,n]) \cdot \widetilde{w}[m,n]. \quad (18)$$

Hence, we have incorporated the weighting of the residual error in order to evaluate the error criterion for coefficient update a step earlier and can express the last line of (10) as

$$2MN \sum_{(m,n)\in\mathcal{L}} \widetilde{w}[m,n]r^{(\nu)}[m,n]\varphi_{M-u,N-v}[m,n] = 2MN \sum_{(m,n)\in\mathcal{L}} r_{\widetilde{w}}^{(\nu)}[m,n]\varphi_{M-u,N-v}[m,n]. \quad (19)$$

3.2. Frequency Domain Representations

In the following we represent all equations in the frequency domain in order to allow an efficient implementation. The equation

$$\sum_{(m,n)\in\mathcal{L}} \widetilde{w}[m,n]\varphi_{u,v}[m,n]\varphi_{k,l}^{*}[m,n] = \widetilde{W}[k-u,l-v]$$

can be expressed as the DFT $\widetilde{W}[k,l]$ of the weighting function $\widetilde{w}[m,n]$ sampled at $[k-u,l-v]$. Hence, we can write the equation necessary for an update with help of (3), (4) and (19) as

$$\Delta c\widetilde{W}[0,0] + \Delta c^{*}\widetilde{W}[2k,2l] \quad = \quad 2MN \cdot R_{\widetilde{w}}[k,l]. \quad (20)$$

Analogously we obtain a second conjugate complex equation. Solving the equations with respect to Δc yields the update equation

$$\Delta c = \begin{cases} MN\frac{R_{\widetilde{w}}^{(\nu)}[u,v]}{\widetilde{W}[0,0]} & , u,v \in \mathcal{M} \\ 2MN\frac{R_{\widetilde{w}}^{(\nu)}[u,v]\widetilde{W}[0,0] - R_{\widetilde{w}}^{*(\nu)}[u,v]\widetilde{W}[2u,2v]}{\widetilde{W}[0,0]^2 - |\widetilde{W}[2u,2v]|^2}, & \text{else} \end{cases} \quad (21)$$

with $\mathcal{M} = \left\{(0,0),(0,\frac{N}{2}),(\frac{M}{2},0),(\frac{M}{2},\frac{N}{2})\right\}$. The case differentiation is necessary due to the symmetry requirements (3), (4), (10) and the definition of $g^{(\nu)}[m,n]$ according to (2).

The basis function with index u,v is selected which maximizes

$$\Delta E_{\mathcal{A}}^{(\nu)} = \begin{cases} 2\frac{R_{\widetilde{w}}^{(\nu)}[k,l]^2}{\widetilde{W}[0,0]} & , k,l \in \mathcal{M} \\ 2\frac{|R_{\widetilde{w}}^{(\nu)}[k,l]|^2\widetilde{W}[0,0] - \mathrm{Re}\{R_{\widetilde{w}}^{(\nu)}[k,l]^2\widetilde{W}^{*}[2k,2l]\}}{\widetilde{W}[0,0]^2 - |\widetilde{W}[2k,2l]|^2}, & \text{else.} \end{cases} \quad (22)$$

The modified residual error used in the approximation is given by

$$R_{\widetilde{w}}^{(\nu+1)}[k,l] = R_{\widetilde{w}}^{(\nu)}[k,l] - \frac{1}{2MN}(\Delta c\widetilde{W}[k-u,l-v] + \Delta c^{*}\widetilde{W}[k-(M-u),l-(N-v)]). \quad (23)$$

The approximation terminates when the decrease of the residual error criterion drops below a prespecified threshold. The parametric model is then obtained by inverse DFT transform

$$g[m,n] = \mathrm{IDFT}\{G[k,l]\}. \quad (24)$$

Finally, the missing block is cut out of $g[m,n]$.

Since all equations can be expressed in the DFT domain, only one transform in the beginning and one at the end is required.

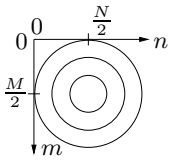

Fig. 3. Isotropic model with circles as loci of constant correlation

4. WEIGHTING BY A CORRELATION MODEL

As already mentioned in Sec. 2, the weighting function allows to assign more importance to certain areas during the approximation, which is not possible in [6]. Generally, the image content of the missing block becomes less correlated to the image content of the surrounding as the distance from the missing block increases. This information is incorporated into the algorithm by the weighting function $\widetilde{w}[m,n]$ given in (8). We suggest an isotropic correlation model given by

$$\rho[m,n] = \hat{\rho}^{\sqrt{(m-\frac{M}{2})^2+(n-\frac{N}{2})^2}} \quad (25)$$

with $\hat{\rho}$ being the correlation coefficient. The loci of constant correlation are circles as illustrated in Fig. 3.

5. SIMULATION RESULTS

In order to evaluate different techniques with respect to their concealment performance, simulated block losses of 8×8 and 16×16 pixels are investigated. Table 1 shows the PSNR results evaluated at concealed blocks. The images Lena, Baboon and Peppers with a size of 512×512 pixels were used for the evaluation.

The principle of the algorithm is summarized with the example of an 8×8 block loss. The missing block and a frame of 7 known pixels form a block of 22×22 pixels according to Fig. 1. The zero-padded block is transformed by the FFT with a size of 32×32. The algorithm terminates when either the termination threshold ΔE_{min} or a maximum number of iterations Max_it is exceeded.

Next, the achieved PSNR gains compared to [6] are described. We choose a fixed set of parameters for an image with a special block loss case but the parameters differ for different images and block loss cases. In [6] the error criterion is evaluated over a fixed rectangular frame like in Fig. 1. The introduced weighting function allows to minimize a weigthed error criterion with respect to the support area. Different correlation models for the weighting function like the isotropic, the separable and a generalised model have shown similar performances. We chose the isotropic model due to slight advantages. The correlation decreases radial symmetrically with distance, e.g. the diagonals are not overrated. Due to weighting the error criterion taking the correlation among pixels into account, considerable PSNR gains from 0.6 dB to 1.8 dB with respect to [6] could be achieved for 8×8 losses. In the case of a 16×16 block loss we obtained similar gains of 0.3 dB to 2.2 dB while using a FFT size of 64×64. Further, in contrary to [6] we were able to halve the FFT size for both loss cases or equivalentely to approximately halve the complexity for the transform and to quarter the number of basis functions to be searched.

In [6] the parameters have to be chosen individually for each image and block loss case. In order to overcome the drawback of no unique parameter set, we are able to provide in contrary to previous work [6] a set suitable for all images belonging to a block loss case. This also means that the disadvantage of selecting an appropriate frame is now overcome. The fixed set of parameters and the achieved PSNR results are given at the bottom of Table 1, resulting in a maximum loss of 0.5 dB with respect to the individual set of parameters. All images presented in this paper are

	8×8 Block loss			16×16 Block loss		
	Lena	Peppers	Baboon	Lena	Peppers	Baboon
Maximally smooth recovery [1]	24.7 dB	26.0 dB	20.0 dB	23.7 dB	24.2 dB	19.5 dB
POCS [3]	24.7 dB	25.7 dB	19.5 dB	22.3 dB	22.1 dB	18.9 dB
Spatial domain interpolation [4]	24.0 dB	26.1 dB	17.8 dB	21.2 dB	23.3 dB	16.4 dB
JPEG Reconstruction [5]	24.5 dB	26.3 dB	18.8 dB	-	-	-
Sequential error-concealment [2]	28.1 dB	29.6 dB	20.6 dB	24.2 dB	26.9 dB	18.8 dB
Frequency-selective extrapolation [6]	26.0 dB	26.4 dB	19.4 dB	22.8 dB	24.5 dB	19.0 dB
Introduced algorithm (individual set of parameters)	27.7 dB	28.2 dB	20.0 dB	24.3 dB	26.7 dB	19.3 dB
Fixed set of parameters: $Max\_it = 11, \Delta E_{min} = 150$	$\hat{\rho} = 0.73$, frame = 7			$\hat{\rho} = 0.74$, frame = 13		
Introduced algorithm (fixed set)	27.3 dB	27.8 dB	19.8 dB	24.2 dB	26.3 dB	18.8 dB

Table 1. Error concealment techniques in comparison.

concealed with the fixed parameter set. Due to the limited space only parts of images are shown (full images can be seen on [7]). Fig. 4 shows on the right hand side the concealed version of the image depicted on the left hand side. Clearly, monotone areas as well as edges of arbitrary orientation can be restored. On the left hand side of Fig. 5 a case of 16×16 block loss is shown and the concealed result is depicted on the right hand side. Noticeably, also the noise-like behavior of the structured fur can be recovered and the subjective result is even more convincing than the PSNR.

In predictive coding like JPEG lost data may lead to consecutive block loss. Fig. 6 considers a case of consecutive 16×16 block loss on the left hand side. The concealing takes place in a block-wise fashion using the already concealed block weighted by 0.1 for concealing the next block. Fig. 6 confirms on the right hand side that also larger block losses can be concealed successfully.

Method [2] has a performance comparable to the introduced algorithm but is computationally expensive. The PSNR gap between [6] and [2] could be closed especially for larger losses. Additionally, [2] has problems in recovering noise like the fur of Baboon which is due to the pixel-based predictive nature of the algorithm.

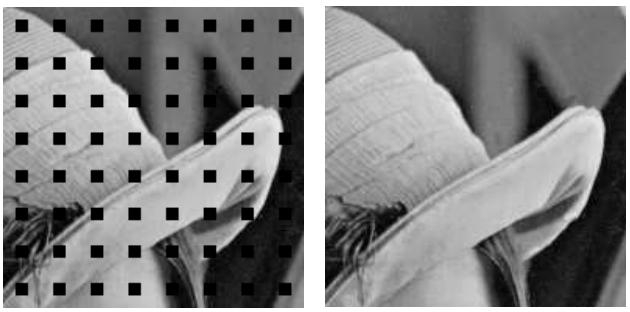

Fig. 4. Left: Simulated 8×8 block loss. Right: Concealed image, iterations: 4.7 per block.

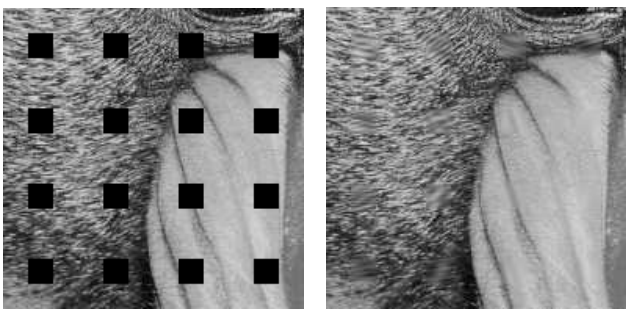

Fig. 5. Left: Simulated 16×16 block loss. Right: Concealed image, iterations: 8.4 per block.

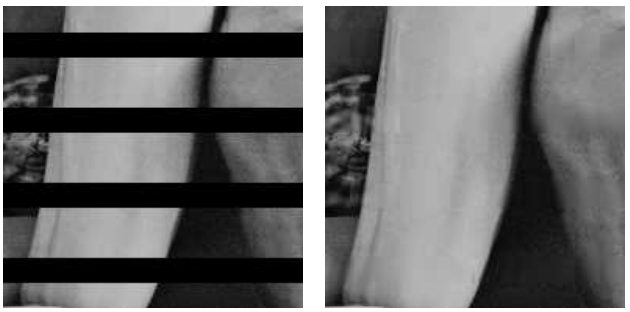

Fig. 6. Left: Consecutive 16×16 block loss. Right: Concealed.

6. CONCLUSIONS

The presented algorithm can conceal monotone areas, edges and also noise-like areas. Considerable PSNR gains could be achieved by incorporating a novel weighted error criterion. Additionally, we are able to present one suitable set of parameters with appropriate results although the individual maximum PSNR results can be achieved for optimized parameters. Future work will concentrate on adaptively choosing the parameters.

7. REFERENCES

[1] Y. Wang, Q.-F. Zhu, and L. Shaw, "Maximally smooth image recovery in transform coding," *IEEE Trans. on Commun.*, vol. 41, no. 10, pp. 1544–1551, Oct. 1993.

[2] L. Xin and M. T. Orchard, "Novel sequential error-concealment techniques using orientation adaptive interpolation," *IEEE Trans. Circuits Syst. Video Technol.*, vol. 12, no. 10, pp. 857–864, Oct. 2002.

[3] H. Sun and W. Kwok, "Concealment of damaged block transform coded images using projections onto convex sets," *IEEE Trans. Image Process.*, vol. 4, no. 4, pp. 470–477, April 1995.

[4] Z. Alkachouh and M. Bellanger, "Fast DCT-based spatial domain interpolation of blocks in images," *IEEE Trans. Image Process.*, vol. 9, no. 4, pp. 729–732, April 2000.

[5] S. Shirani, F. Kossentini, and R. Ward, "Reconstruction of baseline JPEG coded images in error prone environments," *IEEE Trans. Image Process.*, vol. 9, no. 7, pp. 1292–1299, July 2000.

[6] K. Meisinger and A. Kaup, "Spatial error concealment of corrupted image data using frequency selective extrapolation," in *Proc. Int. Conf. on Acoustics, Speech, and Signal Processing (ICASSP)*, Montreal Canada, May 2004.

[7] "http://www.lnt.de/lms/research/projects/concealment/," .